# メカニカルシールにおけるキャビテーション圧力の液種および試験条件による変化

## Variation of cavitation pressure with liquid and operating conditions in mechanical seals

イーグル工業（正）*巻島　創　（正）板谷　壮敏　（正）徳永　雄一郎
九大（正）杉村　丈一
So MAKISHIMA*, Masatoshi ITADANI*, Yuichiro TOKUNAGA*, Joichi SUGIMURA**
*Eagle Industry Co., Ltd. **Kyushu University

Winner of ITC Fukuoka 2023 Excellent Paper Award. Short summary ver. from Tribology Online Vol. 18, No.6 (2023) 436-443.

### 1. Introduction

In order to maintain a stable sealing function of mechanical seals for a long duration, the sliding surface must be protected by forming an appropriate lubricating film between the sliding surfaces. Achieving both sealing and lubrication functions by a mechanical seal is both critical and challenging. To meet these requirements, a new concept of mechanical seals with surface texturing has been developed with grooves and micro-pores, or recesses on a sliding surface[1]. This sealing mechanism uses the negative pressure generated in the diverging gap. Under negative pressure, cavitation is caused by vaporization of fluid or release of gas dissolved in the fluid. Therefore, it is necessary for the designers to estimate the details of the cavitation pressure and the cavitation area for the optimum design of textured mechanical seals.

In our previous study[2], cavitation pressure was measured using a diaphragm-type pressure sensor with micro hole on the sliding surface of the textured mechanical seal. Sliding experiments conducted with water as the sealing fluid showed that the pressure in the cavitation region, $P_{cav}$, depended on the saturated vapor pressure of water. On the other hand, when isopropyl alcohol was used as the sealing fluid, $P_{cav}$ was about 10 kPa higher than the vapor pressure. Even in the same environment, the relationship between $P_{cav}$ and vapor pressure depends on the fluid.

In this study, the measurement of the cavitation pressure $P_{cav}$ in the textured mechanical seal was extended to include some synthetic oils to find a relationship between $P_{cav}$ and the vapor pressure. Furthermore, in order to confirm the effect of sealing gap and the sliding speed, these parameters were changed in experiments. From the obtained results, the mechanism of cavitation pressure determination was investigated.

### 2. Experimental Methods

#### 2.1 Specimens

Figure 1 shows the details near the sliding surface of the mechanical seal used in this study. The stationary ring is made of silicon carbide, which is attached to the fluid bath and pressed against the rotating ring with a spring. The rotating ring is an optical flat made of synthetic glass, which is fixed to a rotating shaft. Textured grooves were produced on a stationery ring surface via laser machining. A pressure measurement hole of a diameter of 0.26 mm was created in the reversed Rayleigh step groove, which was almost perpendicular to the sliding surface. A diaphragm-type pressure sensor with a measurement range of 350 kPa and diameter of 3.8 mm was placed directly below the hole.

Figure 2 shows a schematic of the stationery ring surface. Minimum thickness of the hydrodynamic lubricating film generated by the Rayleigh step, or the minimum distance between two sliding surfaces of mechanical seal, is named the sealing gap. and depends on the depth of the Rayleigh step grooves $D_{RS}$. In the present experiments, $D_{RS}$ of 1.5 μm and 6.0 μm were used in order to see the effect of the sealing gap. As for the reversed Rayleigh step grooves, a depth $D_{RRS}$ of 5.5 μm is employed.

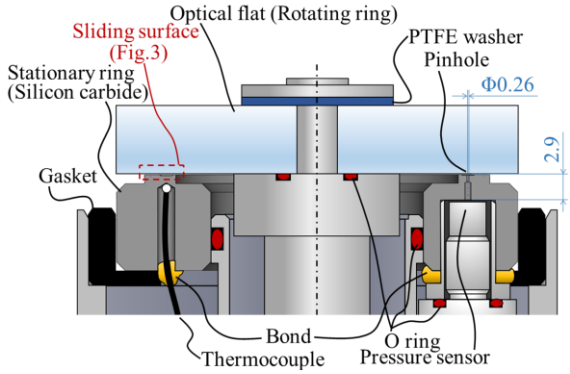


Fig. 1 Details near the sliding surface of the mechanical seal

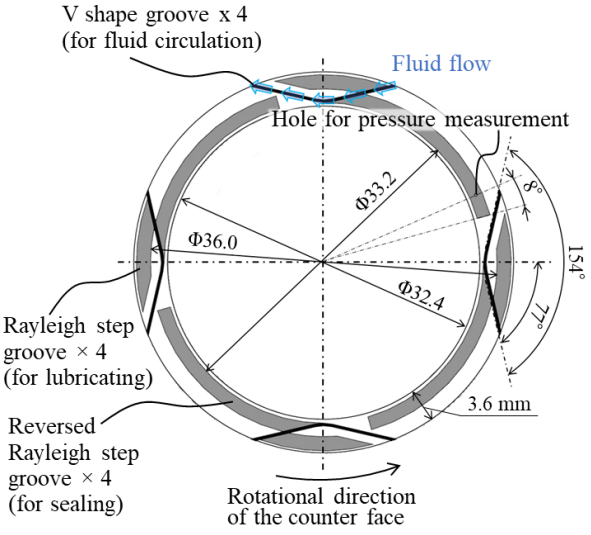


Fig. 2 Dimensions of the textured surface

#### 2.2 Experimental conditions

Table 1 lists the properties of the lubricating oils used in this study. The oils are free of additives. Four oils were selected: non-polar poly-alpha-olefin (PAO), dimethyl siloxane (PDMS) with high gas solubility, and two other polar oils of polyol ester (POE),

Table 1 Test fluids

| Fluid | Kinematic viscosity ($mm^2/s$) | Density ($kg/m^3$) | Vapor pressure (kPa) | Polarity | Air dissolution (mg/L) | Water amount (ppm) |
|---|---|---|---|---|---|---|
| PAO | 19.0 @ 40 °C | 804 @ 25 °C | ＜0.002@100 °C | Non-polar | 115 @ 23 °C | 34 |
| PDMS | 15.6 @ 40 °C | 820 @15.6 °C | ＜0.013@220 °C | Less-polar | 185 @ 23 °C | 99 |
| POE | 19.0 @ 40 °C | 950 @15 °C | ＜0.013@20 °C | Polar | 151 @ 23 °C | 1366 |
| PAG | 18.8 @ 40 °C | 1016 @ 40 °C | — | Polar | 93 @ 23 °C | 541 |

Table 2 Experimental conditions

| | Experiment 1 | Experiment 2 |
|---|---|---|
| Gas condition of fluid before experiment | Air-saturated by bubbling | Degassed by decompressing |
| Sealed fluid | PAO, PDMS, POE, PAG | PAO, PDMS, POE, PAG |
| Load of sliding surface | 47 N | 47 N |
| Rotating speed | 500, 1000, 1500 rpm (0.9, 1.8, 2.8 m/s) | 1500 rpm 2.8 m/s |
| Fluid temperature | 40 °C | 40 °C |
| Pressure | 101 kPa | 101 kPa |

and poly alkylene glycol (PAG).

The experimental conditions are listed in Table 2. In Experiment 1, the cavitation pressure and the dissolved oxygen were measured in the lubricating oils saturated by air bubbling, and the shaft rotation speed was varied from 500 to 1500 rpm, with at least two tests conducted for each speed. Experiment 2 is with degassed oils. The cavitation pressure and dissolved oxygen content were measured once for each degassed lubricating oils at a shaft rotational speed of 1500 rpm. Experiments were conducted with the four oils on the specimen with $D_{RS}$ of 6.0 μm. To confirm the effect of experiments with the $D_{RS}$ 1.5 μm specimen were also conducted with PAO.

## 3. Experimental results

In all experiments, finger cavitation occurred in the inlet area of the reversed Rayleigh step groove immediately after sliding began. Subsequently, the cavitation region expanded to the pressure measurement hole and reached the V-shaped deep groove. There was almost no difference in the appearance of cavitation between Experiment 1 and 2, between lubricating oils, and between different $D_{RS}$.

In all Experiment 1, after the start of rotation, $P_{cav}$ decreased immediately with time and then stabilized. The reason for the changes in $P_{cav}$ with time was that air remained around the pressure sensor before rotating, which was discharged from the pressure measurement hole by the surrounding negative pressure, as reported in our previous study[2]. Figure 3 shows the relationship between $P_{cav}$ and the sliding speed after stabilization for all the oils in Experiment 1. The figure clearly demonstrates that $P_{cav}$ depends on the sliding speed and decreases with the sliding speed.

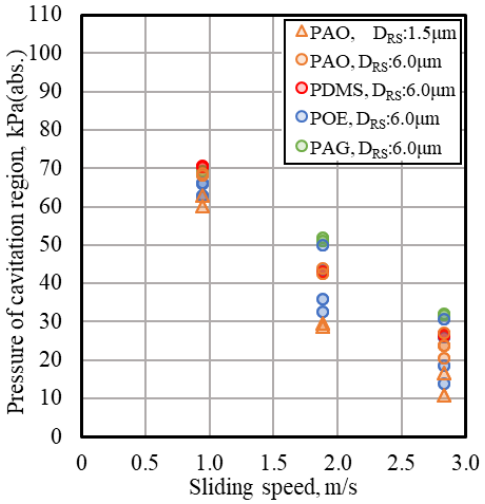


Fig. 3 Variation of $P_{cav}$ with speed for all the oils in Experiment 1

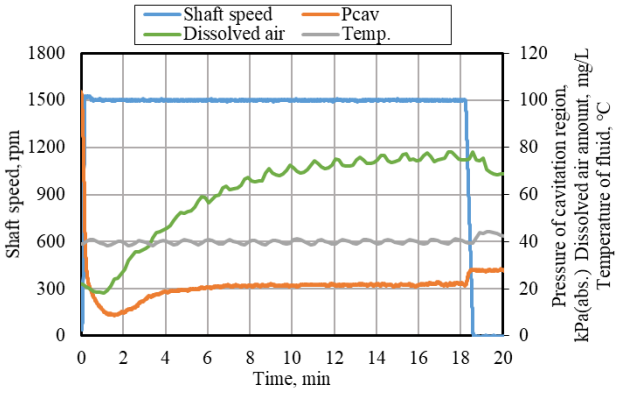


Fig. 4 Pressure measurement result with a $D_{RS}$ of 6.0 μm, rotation speed of 1500 rpm, and PAO; Experiment 2

Figure 4 shows the changes in the shaft speed, $P_{cav}$, the amount of dissolved air and temperature near the sliding surface with time at 1500 rpm with the degassed PAO and the specimen with $D_{RS}$ of 6.0 μm. Similar to Experiment 1, $P_{cav}$ decreased immediately after the start of rotation with time. However, after $P_{cav}$ reached a minimum value of approximately 9 kPa, it began to increase slowly and stabilized at approximately 21 kPa. The amount of the dissolved air was stable at approximately 20 mg/L for a while after the start of rotation, but then it began to increase and stabilized at approximately 75 mg/L after 14 min. This result strongly suggests that $P_{cav}$ increases as the amount of dissolved air increases. In Experiment 2, the similar trends were also observed with the other oils and $D_{RS}$ 1.5 μm.

Figure 5 shows the stabilized value of $P_{cav}$ for the air-saturated lubricating oils and the minimum value of $P_{cav}$ for the degassed lubricating oils at a shaft rotation speed of 1500 rpm. For each lubricating oil, degassed $P_{cav}$ was lower than saturated $P_{cav}$. The

pressure difference between the degassed $P_{cav}$ and saturated $P_{cav}$ depends on the lubricating oil. However, this did not correlate with the amount of dissolved air in each lubricating oil, as listed in Table 2.

## 4. Discussion

In Experiment 1, the cavitation pressure was found to decrease with increasing sliding speed in all oils and sealing gaps. It was found that when the sliding speed was the same, the $P_{cav}$ decreased as the sealing gap was small. In our previous experiments with water[2], the cavitation pressure decreased to approximately the vapor pressure of water. However, in Experiment 1 of this study, all values of $P_{cav}$ did not reach the vapor pressure of the lubricating oil. In contrast to the previous study[2], the $P_{cav}$ was stable and higher than the vapor pressure of each oil in all conditions implying that the formation of cavities was dominated by gaseous cavitation.

In Experiment 2, when the dissolved gases in the lubricating oil were reduced by degassing, the cavitation pressure was lower than that when the lubricating oil was not degassed.

From previous research on cavitation growth[3], cavitation is predominantly vapor cavitation during primary growth, but the dissolved gas is quickly dissipated from the surrounding liquid into the cavitation region, and gaseous cavitation is expected to be dominant. As dissolved gas dissipates from the surrounding liquid into the cavitation region, the cavitation pressure increases. Therefore, theoretically, saturation occurs when the pressure in the cavitation region reaches the dissolved gas partial pressure (atmospheric pressure in this test), and no further dissipation should occur.

However, the experimental results in this study revealed that the pressure in the cavitation region was lower than the atmospheric pressure when saturated. In Experiment 1, fine bubbles separated from the cavitation region in the reversed Rayleigh step groove, suggesting that the same amount of gas dissipating from the surrounding liquid was separated and ejected as a group of fine bubbles. Based on the phenomena suggested by the experimental results, a model of gas absorption and discharge in the reversed Rayleigh step was developed (Figure 6). The amount of gas dissipation and gas emission depends on the sliding environment and the type of fluid, whereas the rate of gaseous cavitation is determined by the sliding conditions and the fluid type. The fraction of gaseous cavitation determines the cavitation pressure, and it is determined according to the different sliding conditions and the fluid types.

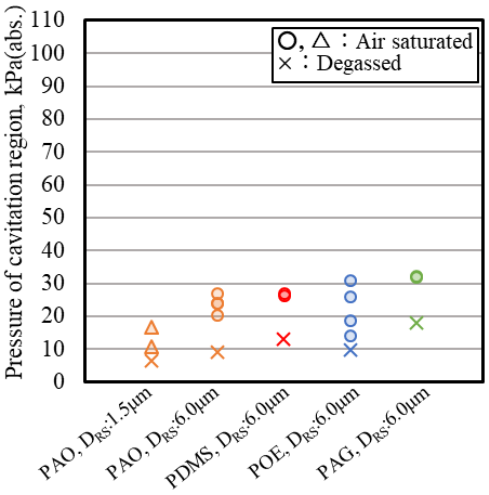


Fig. 5 Cavitation pressure with air saturated and degassed oils

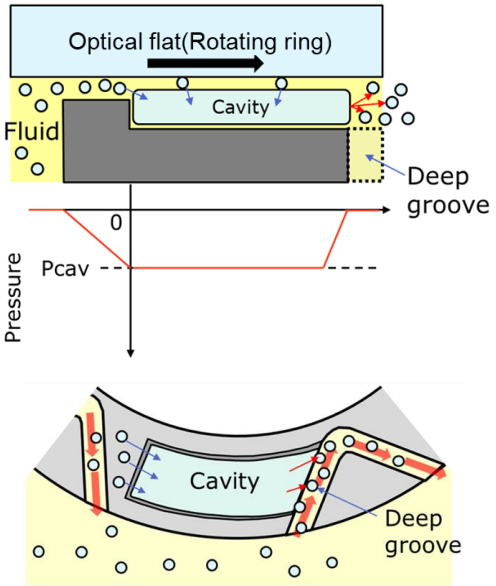


Fig. 6 Model of absorption and discharge of dissolved gas into cavitation

## 5. Conclusions

A series of experiments was conducted to investigate the cavitation pressure and to observe the formation of cavities in a textured mechanical seal. Based on the experimental results, the transportation of gas in and out of a cavity and its relation to the cavitation pressure were discussed, and a model was developed. The following conclusions were drawn:

(1) The cavity pressure $P_{cav}$ decreases with increasing sliding speed in all lubricating oils and all sealing gaps.

(2) With the same lubricating oil and speed condition, thinner sealing gap causes lower $P_{cav}$.

(3) When the sealing gap is the same, $P_{cav}$ at each sliding speed is slightly different depending on the type of lubricating oils.

(4) $P_{cav}$ is low when the amount of dissolved air is small. The effect of the amount of dissolved air on $P_{cav}$ depends on the type of lubricating oil.

(5) In the range of the present experimental conditions, $P_{cav}$ did not approach the saturation vapor pressure of the lubricating oil, suggesting that the cavitation was primarily gaseous cavitation.

## 6. References


1) Tokunaga Y, Inoue H, Okada K, Uemura N, Yamamoto Y. Improvement in Sealing Performance and Friction Reduction by Laser Surface Texturing for Mechanical Seal. In: Proc. 21st Int. Conference Fluid Sealing, 2011. p.91–102.

2) Itadani M, Uemura N, Sugimura J. Observation and pressure measurement of cavitation region in mechanical seal. In: Proc. 25th International Conference on Fluid Sealing 2020, Manchester, 2020, p.45–p.53.

3) Otsu T, Tanaka H, Sugimura J. Initiation and growth of gaseous cavity in concentrated contact in various surrounding gases. Tribology International, 2012;53(9): p.68–p.75.